



Master Degree course in Mechanical Engineering

Master Degree Thesis

Study of a beam with repetitive geometry as filter for desired frequency band

Supervisors

Prof. Alessandro Paolo Daga

Prof. Alessandro Fasana

Ing. Luca Viale

Candidate

Maria Chiara Ceresoli

ACADEMIC YEAR 2024-2025

Acknowledgements

I would like to sincerely thank my supervisors, for their guidance, support, and valuable feedback throughout this research. Their expertise and encouragement have been crucial to the completion of this thesis.

Abstract

The aim of this research is the analysis of a metamaterial tennis racket handle, starting from the maximum simplification as a multiatomic 1D chain to the simulation of the real handle. The latter thanks to its repeated geometry, is capable to behave as a mechanical filter for a specific band of frequency of interest.

Contents

1	Introduction	3
2	Study of the simplified beam	5
2.1	Mass and Stiffness matrices	5
2.2	Transmissibility	6
2.2.1	Transmissibility as ratio between receptances/ numerical calculation	6
2.2.2	Analytical Transmissibility	8
2.3	Metamaterials analysis	10
2.3.1	Multi-modal wave propagation diatomic chain	14
2.4	Trust structure	18
3	Experimental/numerical evaluation	29
3.1	Methodology	29
3.2	Numerical results	29
4	Conclusion	31
	Bibliography	33

Chapter 1

Introduction

The topic of this thesis come from the known problem of epicondylitis, commonly known as tennis elbow, that affect a large number of tennis player, both agonistic and amateur.

It is known that the main cause of this problem in tennis, comes from the transmission of the vibrations generates in the contact between the ball and the rack, which are transmitted from the rack to the player's arm, in particular wrist and elbow.

Assumed the band of frequencies that gives this problem to player as known, the aim of the thesis is to study a simplified structure with repeated geometry, that is able to filter this band of interest, this study can be further develop on a real rack handle. This analysis started from metamaterials theory stated by Léon Brillouin in 1946 in "Wave Propagation in Periodic Structure".

There are different possibilities to create bandgaps in the vibration transmission, affecting the geometry of a structure, the main are reported below:

- Exploiting the bandgap that creates naturally from the repetition of a unitary cell in the structure (Bragg Scattering phenomenon).
- Adding resonators in the structure that creates Locally-resonant Bandgaps (LRBG):
 - Mass-in-mass negative effect density theory
 - Trapping and reradiating of energy

In this study the first approach is chosen.

Chapter 2

Study of the simplified beam

As a first simplification, the rack handle is modeled as a finite chain of masses and springs. The unitary cell initially consists of one mass and one spring, and the cell is repeated the desired number of times. The total number of elements determines the degrees of freedom.

A MATLAB code is implemented to plot transmissibility versus frequency using the characteristics of the unitary cell, enabling the visualization of bandgaps for vibration propagation. This result is compared to the dispersion diagram, also generated through a MATLAB code based on metamaterials theory.

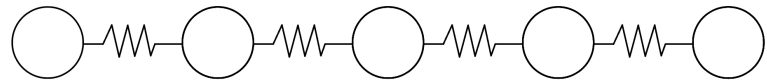


Figure 2.1. ex. 5 repetition of a monoatomic chain

2.1 Mass and Stiffness matrices

The free body diagram of two consecutive masses is analyzed and then extended to the complete chain.

From the mass and stiffness matrices it is possible to extract the natural frequency of the system through the eigenvalue problem. With the eigenvector the modal matrices are calculated and then normalized.

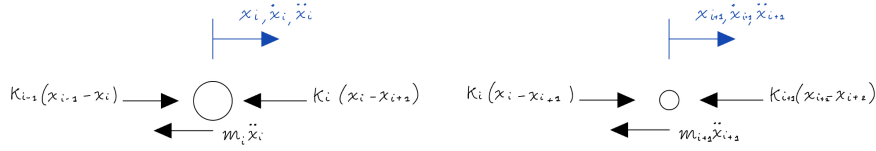


Figure 2.2. Free body diagram

2.2 Transmissibility

The transmissibility represents the ratio between two elements absolute displacements, it is analyzed in this case between the first and the last element of the chain. To calculate it two possible method are considered: numerically or analitically.

2.2.1 Transmissibility as ratio between receptances/ numerical calculation

The receptance of an element in a mdof system represents the displacement of the mass considered due to a force applied only to one mass of the system, that can be itself, autoreceptance, or another one, crossreceptance.

Since the transmissibility represents a ratio between two masses displacement and also the ratio between two receptances, referred to the same force applied, is a ratio between the two displacement, the numerical calculation of transmissibility is performed through the ratio between the two receptance of interest. The receptances α_{11} and α_{end1} are first calculated considering a unitary force applied to the first mass and the ratio between the two is performed.

$$\alpha_{ij} = \Sigma \frac{\varphi_{ir} * \varphi_{jr}}{\omega_r^2 - \Omega^2} \quad (2.1)$$

For example in a 3dof system the receptance of mass 3 due to a force applied on mass 1 is:

$$\alpha_{31} = \frac{\varphi_{31} * \varphi_{11}}{\omega_1^2 - \Omega^2} + \frac{\varphi_{32} * \varphi_{12}}{\omega_2^2 - \Omega^2} + \frac{\varphi_{33} * \varphi_{13}}{\omega_3^2 - \Omega^2} \quad (2.2)$$

While the receptance of mass 1 due to a force applied in 1 is:

$$\alpha_{11} = \frac{\varphi_{11} * \varphi_{11}}{\omega_1^2 - \Omega^2} + \frac{\varphi_{12} * \varphi_{12}}{\omega_2^2 - \Omega^2} + \frac{\varphi_{13} * \varphi_{13}}{\omega_3^2 - \Omega^2} \quad (2.3)$$

The transmissibility from mass 1 to 3 is then:

$$T = \frac{X_3}{X_1} = \frac{\alpha_{31}}{\alpha_{11}} = \frac{\frac{X_3}{F_1}}{\frac{X_1}{F_1}} \quad (2.4)$$

In the following figures are shown the two plots relative to Transmissibility calculated numerical, the first represent the two receptances, first and last masses of the chain, and the other one the transmissibility. The code is run with a 3 masses 3 stiffness unitary cell.

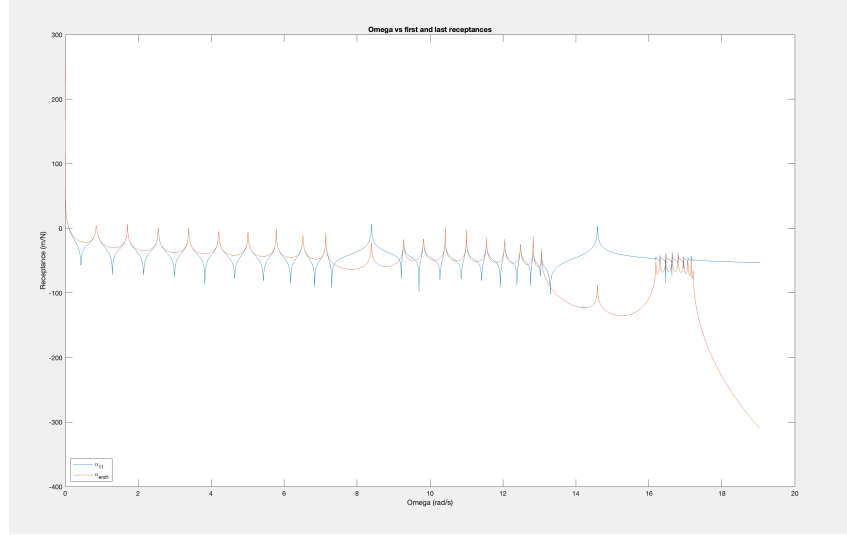


Figure 2.3. Receptances graph

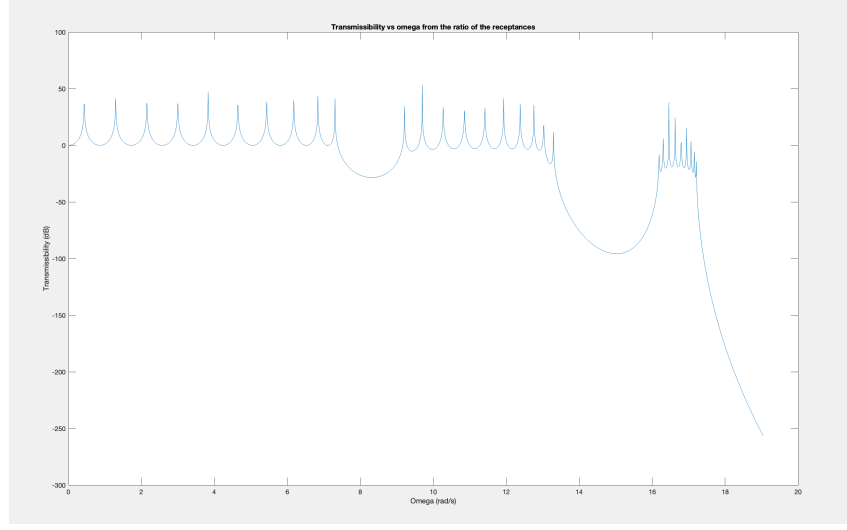


Figure 2.4. Transmissibility graph

In the first image it is easy to recognise the blue curve as the autoreceptance 11, on

mass 1 due to a force applied on the mass 1, this is clear from the presence of antiresonances in between two resonances, not present in the red curve. The second image, representing the transmissibility shows tree bandgaps around 10, 20 and 32Hz frequencies. Increasing the number of different masses or stiffness in the unitary cell it will also increase the number of bandgaps, as the number of degrees of freedom of the unitary cell -1.

2.2.2 Analytical Transmissibility

Another way to get the transmissibility is to perform it analitically since the two recep- tances have the same denominator and the ratio of the two numerators can be simplified as visible in the equations.

$$T = \frac{\alpha_{31}}{\alpha_{11}} = \frac{\varphi_{31}\varphi_{11}(\omega_2^2 - \Omega^2)(\omega_3^2 - \Omega^2) + \varphi_{32}\varphi_{12}(\omega_1^2 - \Omega^2)(\omega_3^2 - \Omega^2) + \varphi_{33}\varphi_{13}(\omega_1^2 - \Omega^2)(\omega_2^2 - \Omega^2)}{\varphi_{11}\varphi_{11}(\omega_2^2 - \Omega^2)(\omega_3^2 - \Omega^2) + \varphi_{12}\varphi_{12}(\omega_1^2 - \Omega^2)(\omega_3^2 - \Omega^2) + \varphi_{13}\varphi_{13}(\omega_1^2 - \Omega^2)(\omega_2^2 - \Omega^2)} \quad (2.5)$$

In the generic for it can be written:

$$T = \frac{\sum \varphi_{3r}\varphi_{1r}(\omega_j^2 - \Omega^2)}{\sum \varphi_{1r}\varphi_{1r}(\omega_j^2 - \Omega^2)} \quad (2.6)$$

With $j = 1, \dots, ndof, j \neq r$

As before an example of a 3 elements cell is represented in the code.
In the images below the script and the plot of transmissibility versus frequency, the graph is the same as the one obtained numerically.

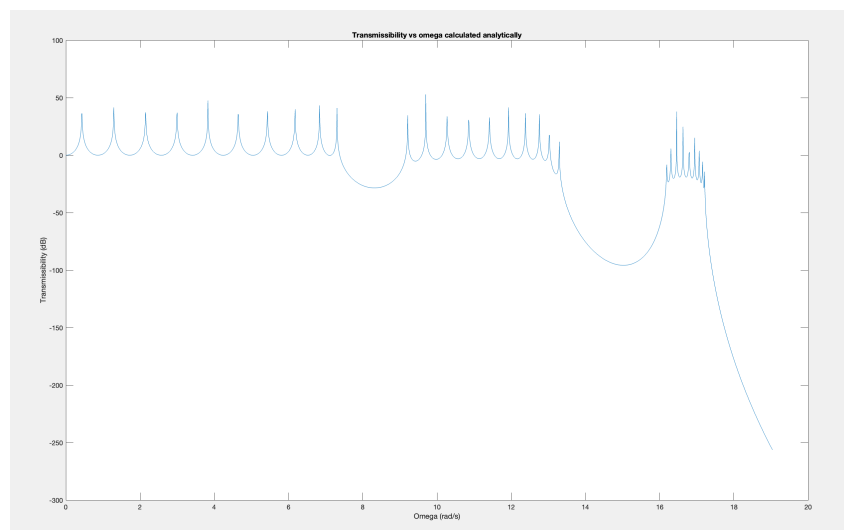


Figure 2.5. Analitical transmissibility graph

2.3 Metamaterials analysis

In this section the chain is analyzed as infinite. As a first simplification an infinite monoatomic chain is considered. the wave propagation can only happen for wavelengths (λ) bigger than 2 times the distance between the masses (d).

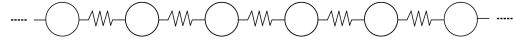


Figure 2.6. Infinite chain

The periodicity of the wave can be defined in frequency through $\lambda = \frac{1}{a} = \frac{2\pi}{K}$ and in time through the period $T = \frac{1}{\lambda}$. In which a is the number of cycles per unit space and K is defined as $K = \frac{2\pi}{\lambda}$.

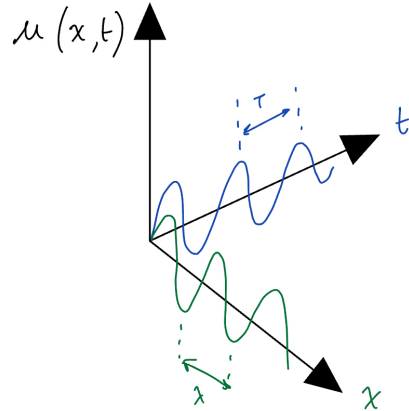


Figure 2.7. Periodicity in time and space

From d'Alembert, the propagation of a 1D wave in space and time, for continuous and discrete ($x_n = nd$), can be written as:

$$u(x, t) = A e^{i(\omega t - Kx)} \quad (2.7)$$

$$u(x_n) = A e^{i(\omega t - K n_n)} \quad (2.8)$$

It is now necessary to define a nondimensional wave number $\xi = Kd$ and introduce it in the previous equations, that becomes:

$$u(x, t) = A e^{i(\omega t - n \xi)} \quad (2.9)$$

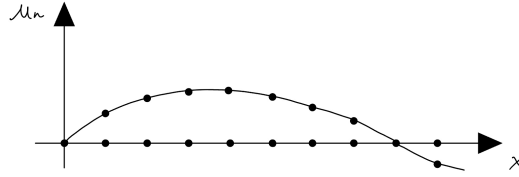


Figure 2.8. Wave propagation in discrete

While all the masses vibrate at the same frequency ω they differ from a phase term that depends on the non-dimensional number and the position of the mass in the chain. $\omega t - n\xi$ represent the phase delay of the time harmonic oscillation. It is possible to relate one mass position to its subsequent or its precedent through the Bloch condition, named after the physicist who studied this phenomenon.

$$u_{n+1} = u_n e^{-i\xi} \quad (2.10)$$

$$u_{n-1} = u_n e^{i\xi} \quad (2.11)$$

Since $u_n(\xi)$ is periodic in ξ with period 2π , it is possible to only study the interval $-\pi \leq \xi \leq \pi$ and since $\xi < 0$ represent the left going wave while the $\xi > 0$ the right going wave, knowing this a priori and assuming symmetry around 0, true in most scenarios, the domain analyzed can be restricted to $\xi \rightarrow [0, \pi]$. The two extreme cases are:

- for $xi = 0 \rightarrow u_{n+1} = u_n$ in phase motion.

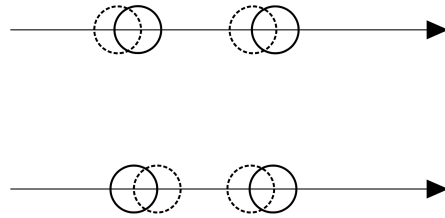


Figure 2.9. In phase and out of phase

- for $xi = 0 \rightarrow u_{n+1} = -u_n$ opposition of phase motion.

Considering the unitary repetitive cell as a mass (m) and stiffness γ , the free body diagram and equation of motion can be written for time domain as:

$$m\ddot{u}_n + \gamma(u_n - u_{n-1}) + \gamma(u_n - u_{n+1}) = 0 \quad (2.12)$$

And in frequency domain:

$$-m\omega^2 u_n + 2\gamma u_n - \gamma u_{n-1} - \gamma u_{n+1} = 0 \quad (2.13)$$

That with the Bloch condition for mass preceding and following in the chain becomes.

$$-m\omega^2 u_n + 2\gamma u_n - \gamma u e^{i\xi} - \gamma u_n e^{-i\xi} = 0 \quad (2.14)$$

$$-m\omega^2 + 2\gamma - \gamma(e^{i\xi} - e^{-i\xi}) = 0 \quad (2.15)$$

It is possible to notice that the part between brackets is replaceable with $2\cos\xi$, and this easily becomes the dispersion relation after few passages:

$$\omega^2 = 2\frac{\gamma}{m}(1 - \cos\xi) \rightarrow \omega = \sqrt{2\frac{\gamma}{m}(1 - \cos\xi)} \quad (2.16)$$

In particular the second expression describes a periodicity of ω in ξ of period 2π . This graph can be analyzed only in the interval $[0, \pi]$ due to the periodicity and this interval that fully describes all spectral scenarios is called the irreducible Brillouin zone, IBZ.

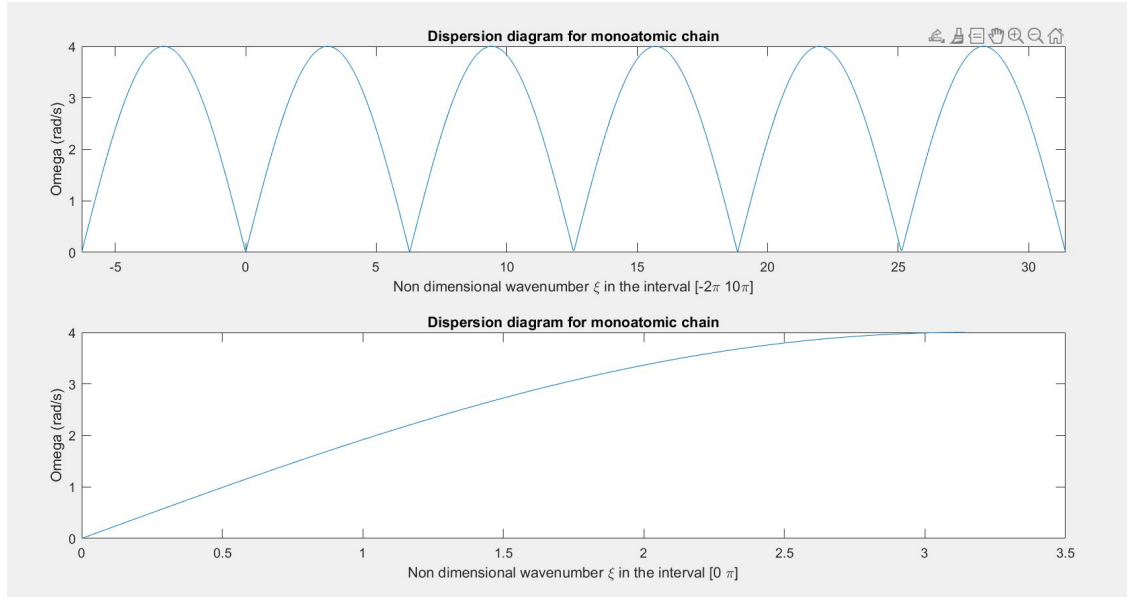


Figure 2.10. Monoatomic chain behaviour

It can be generalized even more introducing the monodimensional frequency $\Omega = \frac{\omega}{\omega_0}$, with $\omega_0 = \sqrt{\frac{\gamma}{m}}$, $\Omega = \sqrt{2(1 - \cos\xi)}$. The graph is now always limited at $\Omega=2$.

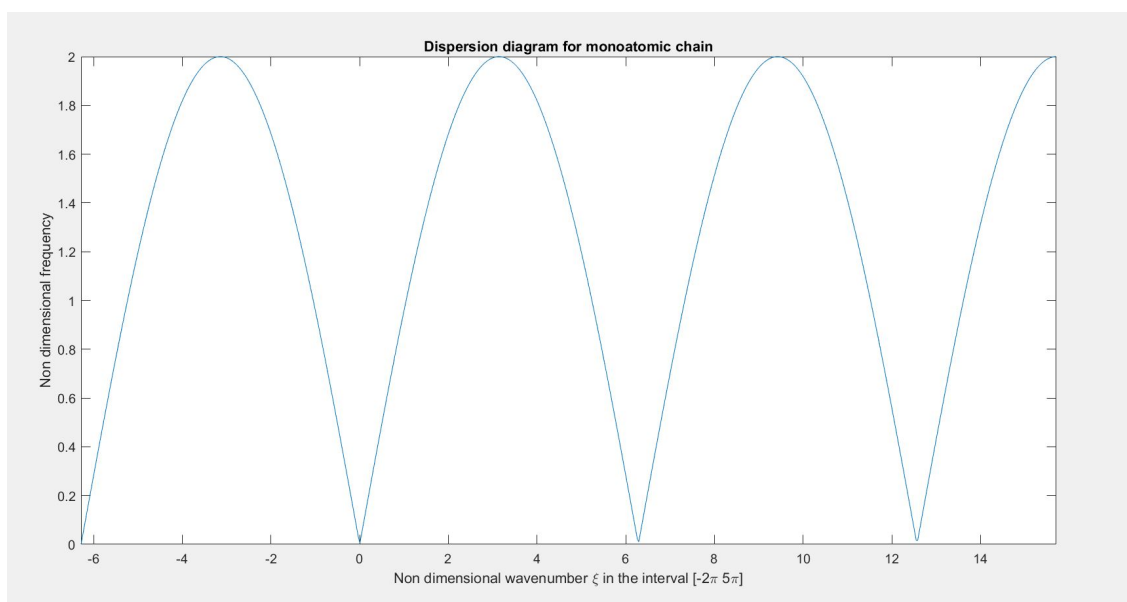


Figure 2.11. Non dimensional frequency

2.3.1 Multi-modal wave propagation diatomic chain

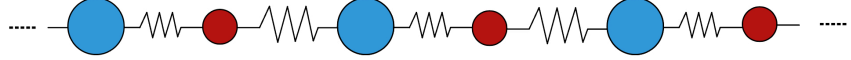


Figure 2.12. Diatomic chain

Extending the solution to the diatomic chain and solving the equation of motion adding the propagation Bloch condition.

$$\begin{cases} -m_1 \ddot{u}_{1n} - \gamma_1(u_{1n} - u_{2n}) - \gamma_2(u_{1n} - u_{2n-1}) = 0 \\ -m_2 \ddot{u}_{2n} - \gamma_1(u_{2n} - u_{1n}) - \gamma_2(u_{2n} - u_{1n+1}) = 0 \\ u_{1n+1} = e^{-i\xi} u_{1n} \\ u_{2n-1} = e^{i\xi} u_{2n} \end{cases}$$

it then becomes, written in matrix form:

$$\begin{bmatrix} m_1 \omega^2 + (\gamma_1 + \gamma_2) & -(\gamma_1 + \gamma_2 e^{i\xi}) \\ -(\gamma_1 + \gamma_2 e^{-i\xi}) & m_2 \omega^2 + (\gamma_1 + \gamma_2) \end{bmatrix} \begin{bmatrix} u_{1n} \\ u_{2n} \end{bmatrix} = \begin{bmatrix} 0 \\ 0 \end{bmatrix}$$

Setting the determinant of the matrix equal to zero, the two roots and two wave modes are obtained.

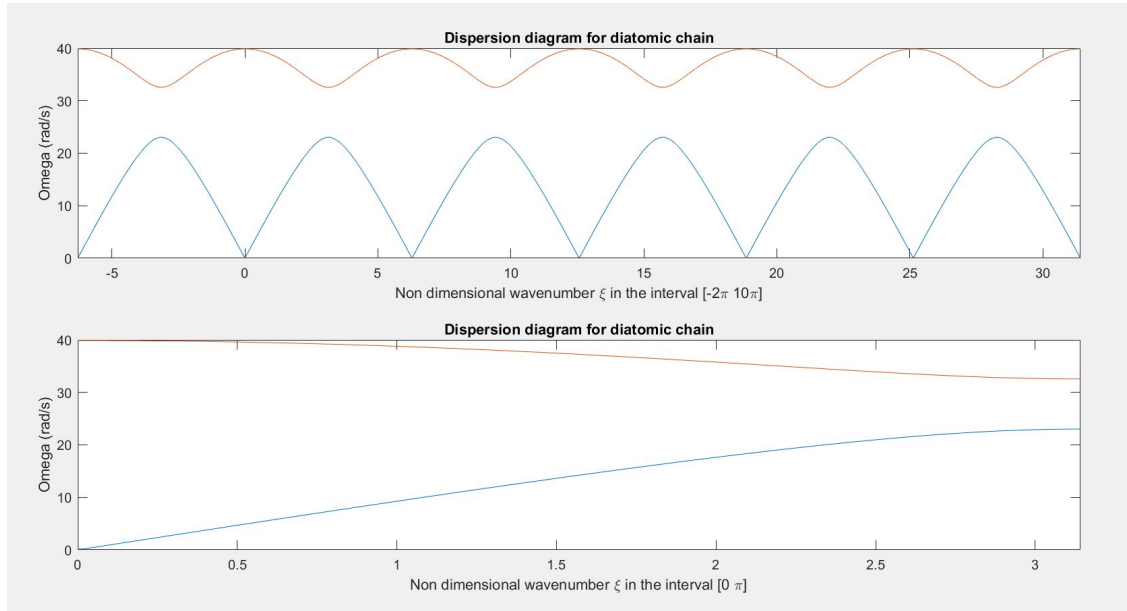


Figure 2.13. Diatomic chain behaviour

Multi-modal wave propagation n-atomic chain

It is possible to extend the calculation to a multiaatomic chain. Hereafter the generic stiffness matrix for the unitary cell.

$$\begin{bmatrix} -(\gamma_1 + \gamma_{end}) & \gamma_1 & 0 & \dots & 0 & \gamma_{end}e^{i\zeta} \\ \gamma_1 & -(\gamma_2 + \gamma_1) & \gamma_2 & 0 & \dots & 0 \\ \dots & & & & & \\ \gamma_1e^{-i\zeta} & 0 & 0 & \dots & \gamma_{end-1} & \gamma_{end} + \gamma_{end-1} \end{bmatrix}$$

While the mass matrix is just a diagonal matrix of the masses of the unitary cell, the stiffness matrix is similar to the one of mdof for a single cell, with the singularity of two elements: the last element of the first row is in fact $\gamma_{end}e^{i\zeta}$, while the first element of the last row is now $\gamma_1e^{-i\zeta}$ for a generic unitary cell stiffness vector going from 1 to end.

In the example the repeated cell analyzed is composed by four different masses and stiffness for simplicity but any number of elements can be chosen for the calculation.

Here after the obtained result of the dispersion diagram, the two axes are now switched to get an easier comparison with the dispersion diagram.

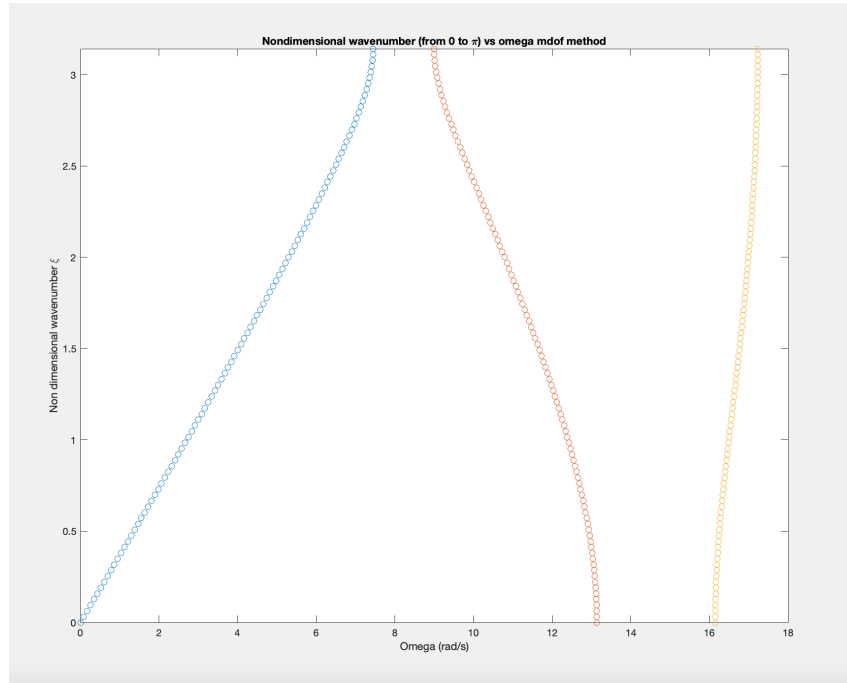


Figure 2.14. Dispersion diagram for three-atomic cell

It is of particular interest the confrontation of the dispersion diagram, from metamaterials

theory, and the transmissibility plot of mdof model. The two models, if the transmissibility refers to a chain with enough repetitions, show the same bandgaps.

It is easy to see how the more repetitions are performed and the more the solution given by transmissibility analysis is close to the solution of the dispersion diagram for an infinite chain. In particular here is show that the 2 repetitions model gives a solution where the bandgaps are not detectable, 4 repetitions already shows a better approximation of the solution and 8 repetitions are definitely enough for a good representation of the infinite fenomenon.

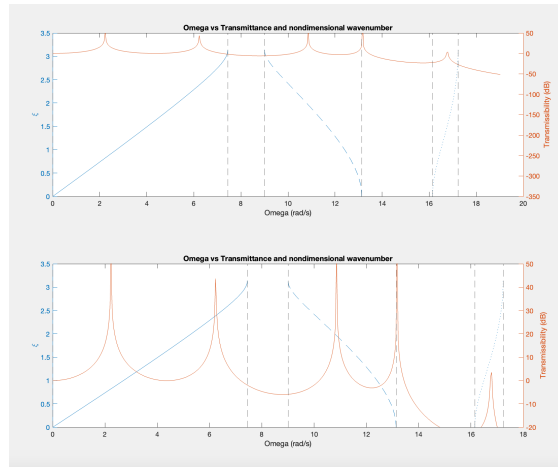


Figure 2.15. 2 repetition of the unitary cell

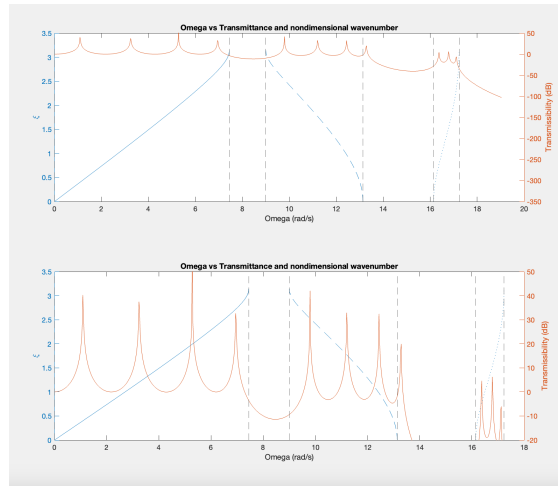


Figure 2.16. 4 repetition of the unitary cell

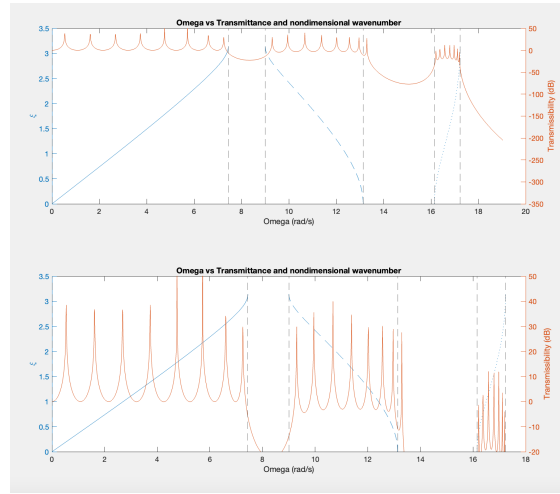


Figure 2.17. 8 repetition of the unitary cell

In those bands, no wave mode is available because no real eigenvalue of the ξ -dependent eigenvalue problem can be found. The bandgaps number increase with the number of masses or stiffness in the unitary cell.

2.4 Trust structure

Until now the elements considered were only mass and stiffness while from now on all the beams are considered as trust structure, in which the beam mass is divided in two half and positioned at the extremities of the beam. The stiffness is $\frac{EA}{l}$, where E is the Young modulus, A the section area and l the length of the beam. The trust structure theory, unlike Euler Bernulli theory, only takes into account of the traction and compression stress.

Case 1D analysys

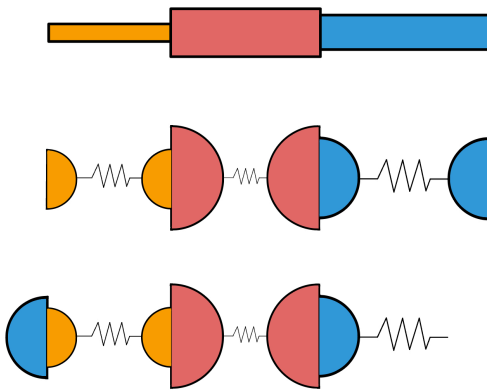


Figure 2.18. Trust structure for 1D

Initially, the one-dimensional case is considered, which does not differ significantly from the previous examples.

Since the mass of the beam is not concentrated in a single node, it is crucial to determine how to distribute the unit cell masses. The most effective solution is to divide the mass of each beam in half and assign it to the nodes at the two ends of the beam.

Particular attention must be given to the first and last nodes of the cell. Two main options are available:

The first option is to leave the starting and ending half-masses in the first and last nodes, as shown in the first example. The second option is to shift the last half-mass to the first node and sum it to the half mass of the first beam, as illustrated in the second sketch. Since the two structure are equivalent, both approaches yield the same results.

Both methodologies are suitable for studying transmissibility and the dispersion diagram, but for this analysis, the first approach has been chosen for the transmissibility study because it provides a more accurate representation of reality. In this approach, the chain is considered finite, and the extremities are represented in their actual positions.

On the other hand, the second approach is used for the dispersion diagram analysis, as it assumes the chain is infinite, making the position of the extremities irrelevant.

This assumption simplifies the calculations by reducing the number of masses by one. In this configuration, the fourth node becomes the subsequent node in the chain and is represented using the well-known Bloch formulation, which accounts for the periodic behavior of an infinite system.

For the two cases the mass matrix is composed by all the nodes masses calculated and then diagonalized. Regard the two stiffness matrices are obtained in a similar way to mdof method. Below are represented the graphs relative to a 4 beam cell with different characteristics.

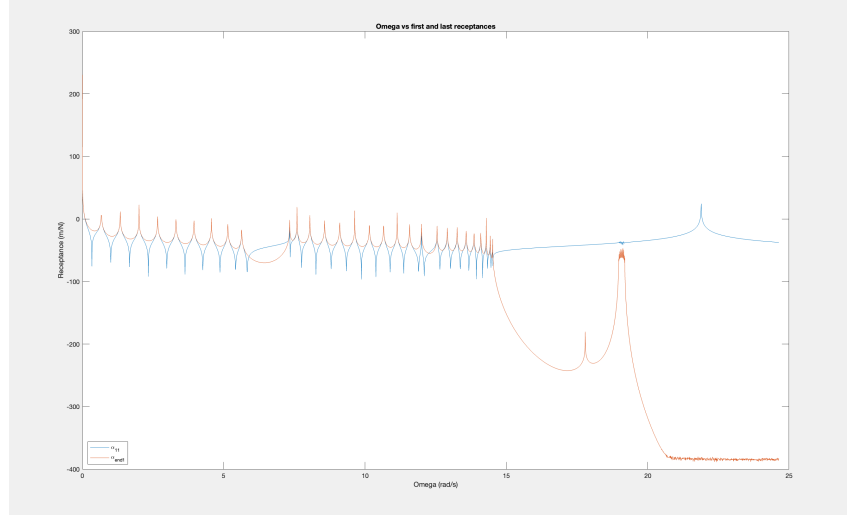


Figure 2.19. First and last receptances plot

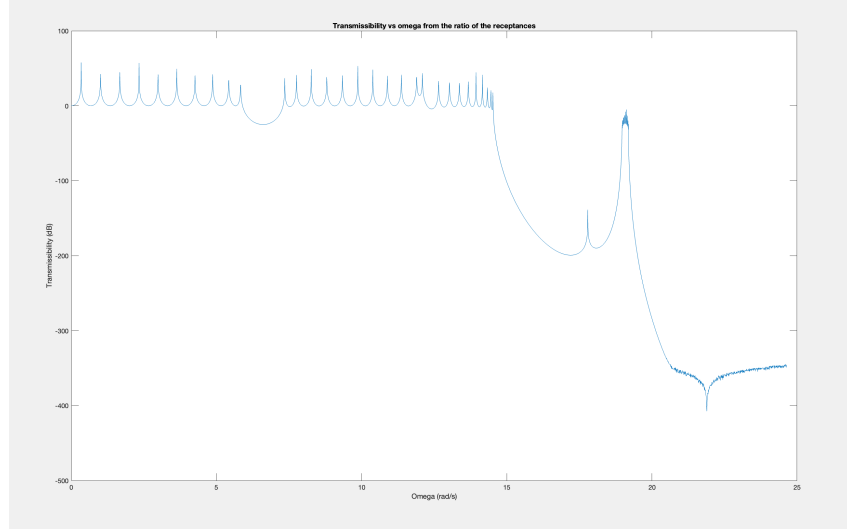


Figure 2.20. Transmissibility plot

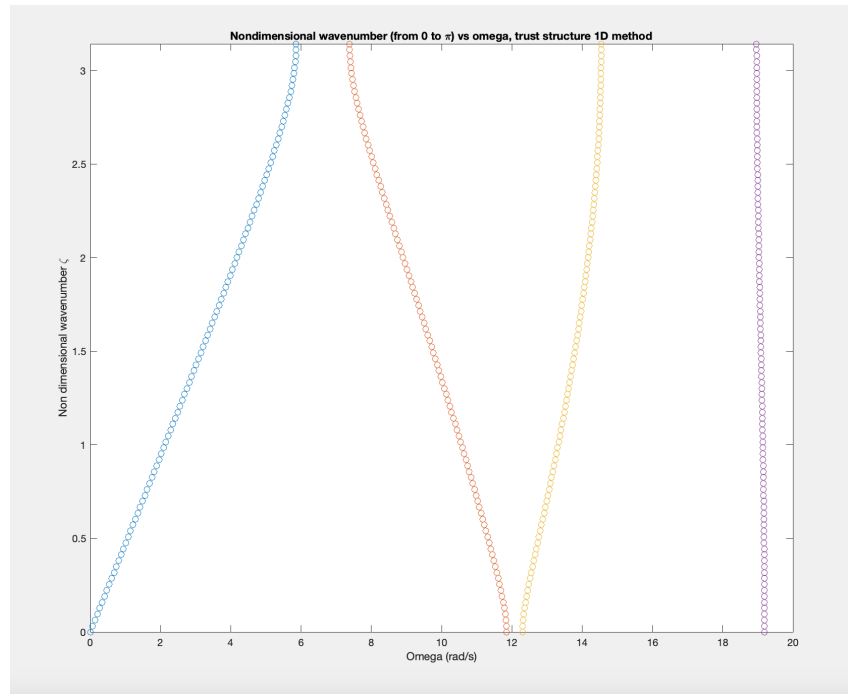


Figure 2.21. Dispersion diagram plot

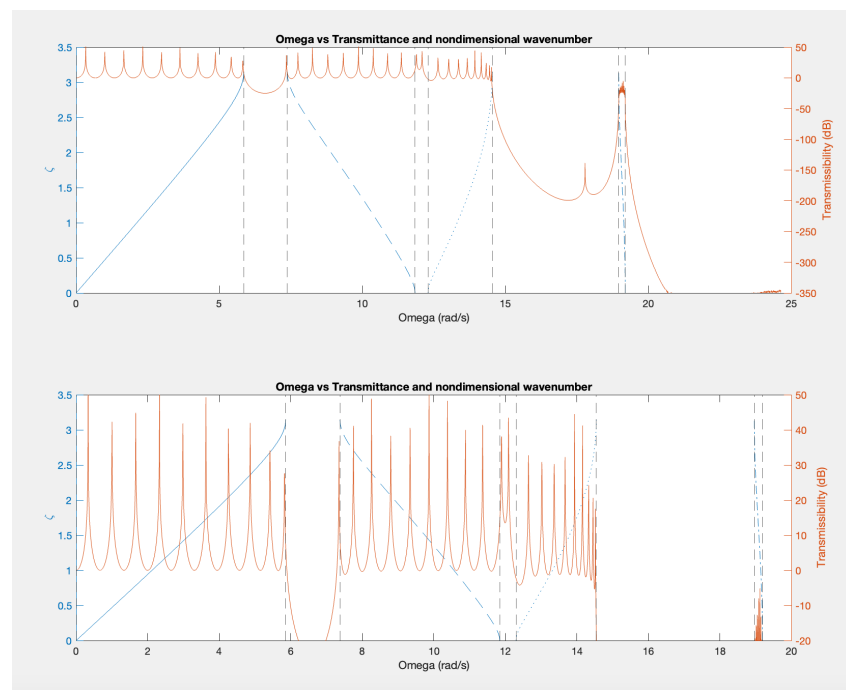


Figure 2.22. Correspondance between transmissibility and dispersion diagram

Case 2D

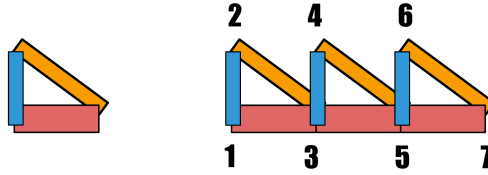


Figure 2.23. Example 2D unitary cell

The analysis becomes more complex when extending the structure to two dimensions. For each beam, it is necessary to consider the tensile and compressive forces acting along the two axes of the global coordinate system. To achieve this, the displacements of the masses must be decomposed into their components, u_x and u_y .

Since the beams can assume any possible orientation, the displacements of the masses in local coordinates (relative to each beam) must first be converted into the global coordinate system. To accomplish this:

A local stiffness matrix is calculated for each beam, representing its behavior in local coordinates. This matrix is then multiplied by a rotation matrix to transform it into the global coordinate system. This process results in the beam's behavior being expressed in global coordinates. The transformed stiffness matrix can then be properly placed into the global stiffness matrix, reflecting the beam's correct position and orientation in the overall structure.

The numbering of the nodes is not as straightforward as in the previous case. Therefore, it is arbitrarily chosen that the node numbering increases along the x-direction, and for nodes with the same x-coordinate, the numbering increases along the y-direction.

This type of numbering results in a sparse stiffness matrix, as nodes that are physically close to each other may have node numbers that are numerically far apart.

The analysis is conducted with the unit cell repeating only in the x-direction.

Three matrices are created to organize the necessary information:

- A matrix containing the coordinates of each node;
- A matrix specifying which nodes are associated with each beam;
- A matrix indicating which last node(s) of one unit cell are also considered the first node(s) of the subsequent repetition (this can include multiple nodes).

For the formulation of the mass matrices, the process of distributing the masses among the nodes is better illustrated in the accompanying image. The same reasoning applied in the 1D case is used.

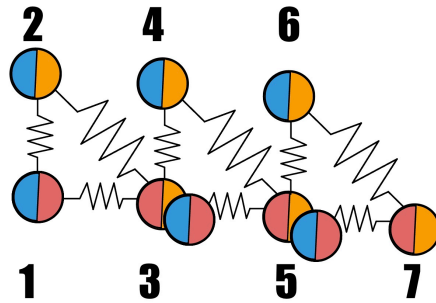


Figure 2.24. Example of 3 repetition structure for Transmissibility

For the dispersion diagram, the logic was to "move" the mass of the common node(s) on the right (which corresponds to the left common node(s) of the following cell) and sum it with the mass of the common node(s) on the left.

The common nodes on the right effectively become the "virtual" nodes of the subsequent repetition, described by the Bloch condition.

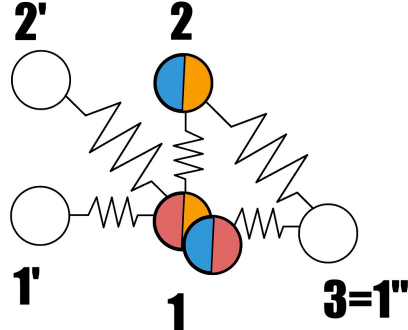


Figure 2.25. Cell structure for dispersion diagram

During the study, it became evident that any complex structure can have multiple ways of representing the unitary cell. However, all representations should lead to the same result, as they describe the same structure. The case in question is illustrated in the image below: The three cell structures are equivalent but one is actually represented not isostatic, however it represents a problem only in the last repetition of the cell.

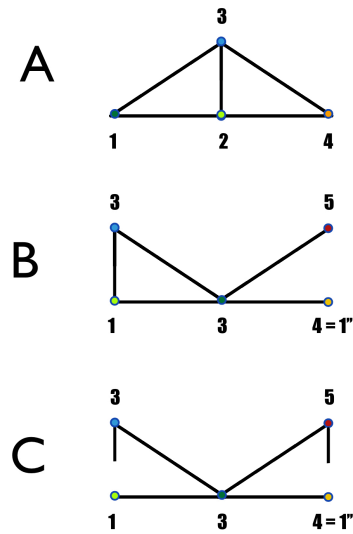


Figure 2.26. Example of three equivalent structure

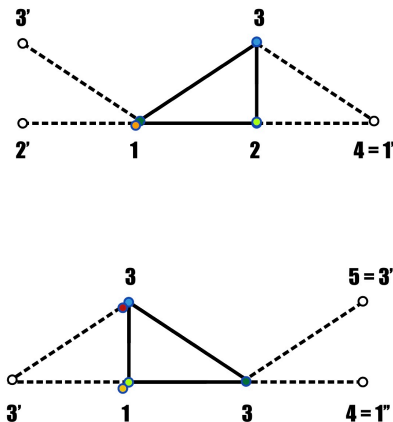


Figure 2.27. Unitary cell for dispersion diagram

Further validation of this method and the calculations was performed by reducing the structure to a 1D system and validating it against the codes for 1D trust structures and MDOF systems.

Regarding transmissibility, another important aspect of comparing equivalent structures is ensuring that the response of the system is calculated in the same nodes. For this reason, it was necessary to perform one additional repetition for the butterfly-like structure compared to the triangular one.

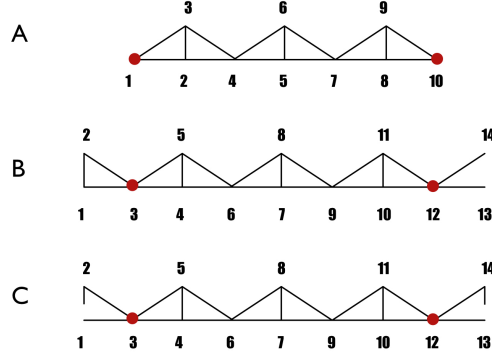


Figure 2.28. Number of repetition for confrontation

Results for 2D Trust Structure Transmissibility

Hereafter the results for Transmissibility relative to the three equivalent structures mentioned before. Respectively the graphs represent the structures in the order A, B and C. In this case, the transmissibility is analyzed along the x-axis, but the same reasoning can be applied to the y-axis.

Than the three graph overlapped:

It is evident that the three structures exhibit the same potential bandgaps. It is important to compare these results with the dispersion diagram to verify the identified bandgaps. For the comparison the Structure A has been selected.

Results for 2D Trust Structure dispersion diagram

The image below show the dispersion diagram for the three structures. While the transmissibility analysis showed slight differences between the three curves, in this case, the curves related to x-axis transmission are identical for all three structures and are presented as follows:

Comparison between the two method

The comparison between transmissibility and dispersion diagram is made by overlapping the two graphs. It is evident that the two methods lead to the same solution, identifying bandgaps at the same frequencies.

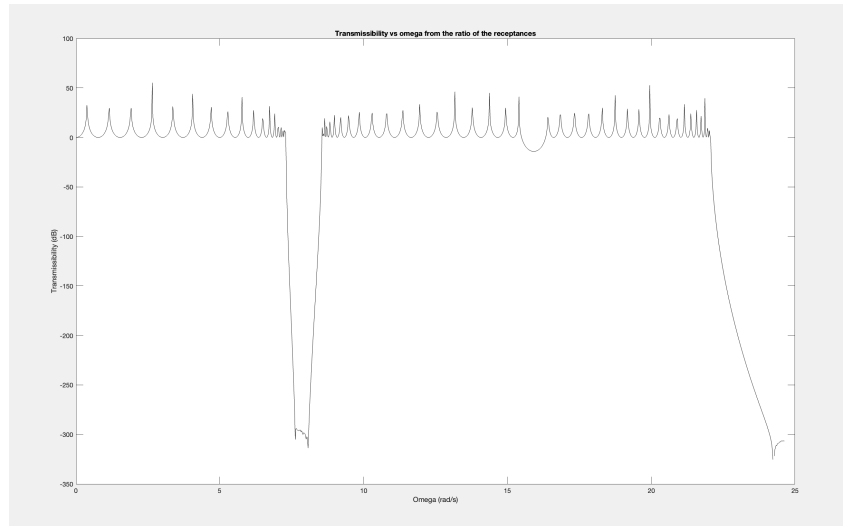


Figure 2.29. Structure A

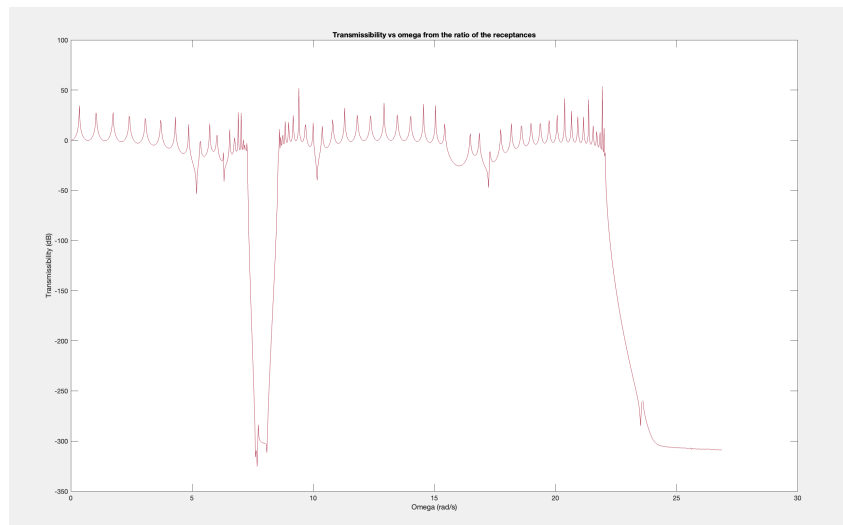


Figure 2.30. Structure B

2.4 – Trust structure

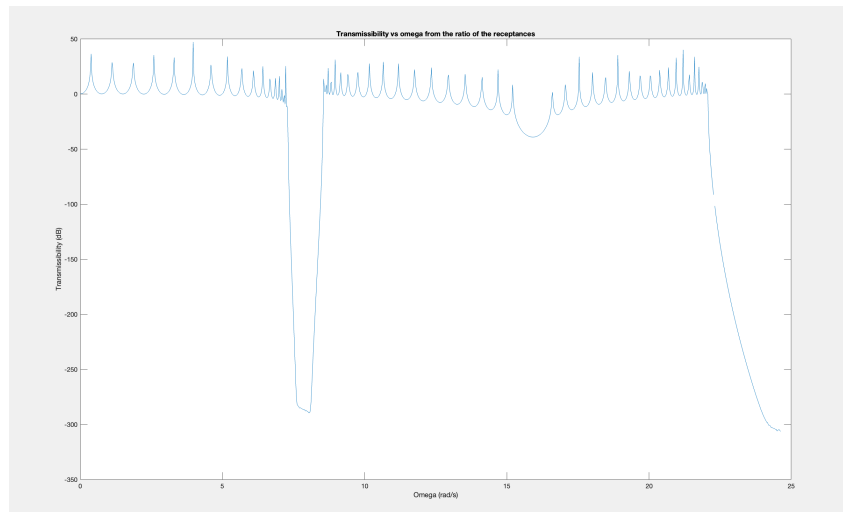


Figure 2.31. Structure C

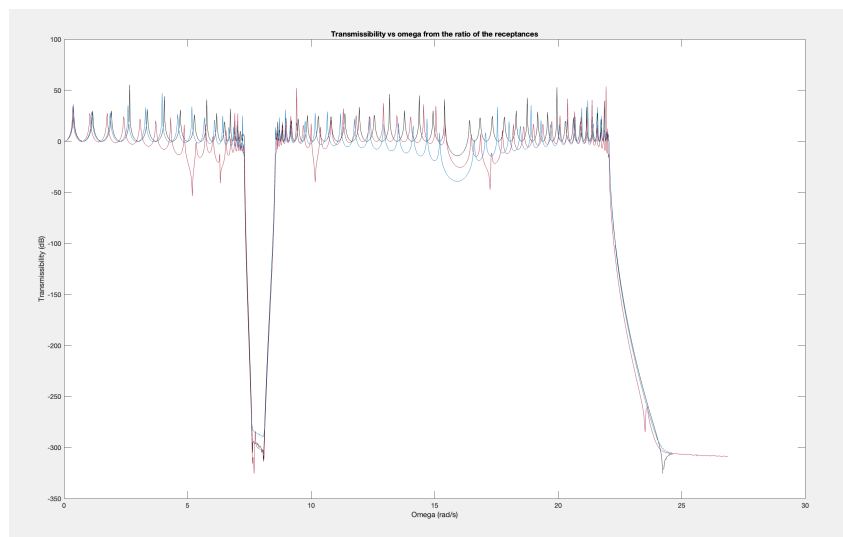


Figure 2.32. Graph of the three structures overlapped

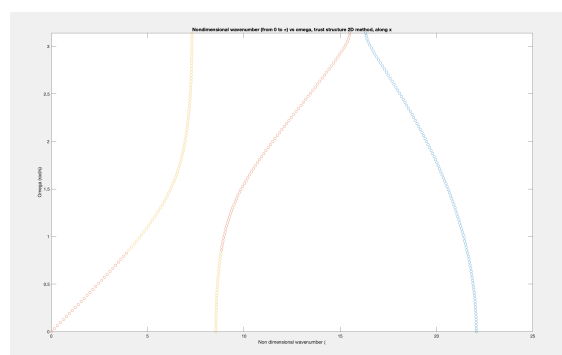


Figure 2.33. Dispersion diagram on x

Bibliography